Design of a Simple Feeding Network for 5G Multidirectional Antennas

Giovanni Maria Schettino, Fulvio Babich, Giulia Buttazzoni
Department of Engineering and Architecture (DIA)
University of Trieste, Italy
E-mail: giovannimariaschettino@gmail.com,{babich,gbuttazzoni}@units.it

***Abstract*—Multidirectional antennas are one of the enabling technologies for the widespread diffusion of intelligent vehicles, which are expected to fill smart cities in the near future characterized by the fifth generation cellular system (5G). In this context, this paper proposes a simple and versatile design procedure for a feeding network, that realizes the beam steering of linear antenna arrays. The developed procedure is intended for a feedline, which must meet some requirements typical in a 5G scenario, such as, for example, easy mass production, low cost, easy integration with other system components and compactness. Precisely, a Blass matrix using the microstrip technology and identical branch line directional couplers is implemented, so that the multidirectional antenna system can be entirely printed on a compact and cheap printed circuit board (PCB). However, when the coupling value is fixed in advance, some pointing directions may be not realizable. So, this paper proposes an algorithm, which evaluates a desired number of beams, in such a way to have a simple design procedure of a feeding network for a multidirectional linear antenna array. The effectiveness of the developed solution is validated by numerical results.**

***Index Terms*—5G, Antenna array, beamforming network, Blass-matrix, branch line directional coupler.**

I. Introduction

Compared to previous communication standards, the fifth generation (5G) system has revolutionized the concept of the mobile network. In fact, 5G is a new global wireless standard, which has been developed to enable a new type of networks, designed not only to improve communication standards, but also to offer new services, such as, for example, remote healthcare, precision agriculture, digitalized logistics, factory automation. In the smart cities of the near future, the goal is to connect everyone and everything together, including machines, vehicles, objects and devices [1]. Of course, the feasibility of such a challenging goal depends on technological aspects. To deliver the desired services, the new technology must support a higher data transmission rate, an increased spectral and energy efficiency, an improved signal-to-interference-plus-noise ratio. So, the evolution of 5G wireless systems has pushed to adopt new frequencies in the millimeter wave (mm-Wave) spectrum. But, at these frequencies, along with the advantages (mainly related to the broad spectrum available), there are also many limitations, such as greater path losses, possible shadowing, rain attenuation and molecular absorption. Moreover, as new frequencies are explored, new path loss models and channel characterizations are required [2]–[4]. In addition, a fundamental change is expected in 5G systems,

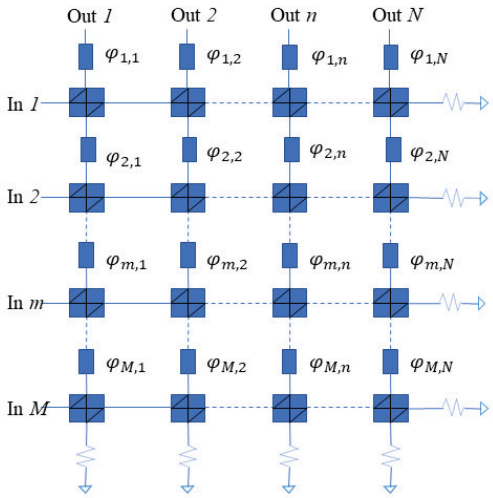

Fig. 1. Blass matrix scheme.

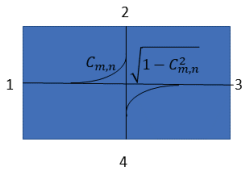

Fig. 2. Directional coupler scheme.

where the coexistence of two types of path is foreseen, namely a macro-based mobile telecommunication path and a local-based mobile telecommunication path. Along with the challenges of the need for adequate coordination, this change should allow a significant cost relaxation [5].

Within this context, antenna arrays with beam steering capabilities have become increasingly important, thanks to the potential that makes them the ideal candidate to ensure the desired performance, such as, for example, high throughput, high capacity and low latency [6]–[24]. Multibeam antennas capable of generating a number of beams are the key hardware to enable the diffusion of 5G systems. In particular, passive multibeam antennas are interesting, as they perform beam-forming in the radio frequency (RF) domain without any active component. Of course, passive multibeam antennas require

an adequate feeding technique. The most common solutions found in the literature are based on the Butler matrix [25], [26], on the Blass matrix [27]–[29], on the Nolen matrix [30], [31] and on the Rotman lens [32], [33]. Interestingly, [34], [35] offer detailed reviews of different feeding techniques specifically adopted in 5G applications.

This paper proposes a new design method for a passive beamforming network that implements a Blass matrix, which is intended to be fully integrated with a linear antenna array on a single substrate. This is very attractive for future 5G applications, as the resulting structure is easy to manufacture, inexpensive, compact, has a very low profile and can be easily integrated with other devices. The proposed feeding network implements the phase distribution through phase shifting microstrip transmission lines and directional couplers. In particular, here, the branch line is assumed as directional coupler, which makes the structure very simple and versatile. However, it is shown in the paper that, when the coupling value is fixed in advance, the beam feasibility is not ensured and an algorithm is proposed to find a number of feasible pointing directions.

The remaining of this paper is organized as follows. Next section introduces the Blass matrix concept and the principle of operation. Then, Section III describes the developed design procedure, which is validated by a numerical example proposed in Section IV. Finally, Section V summarizes the most relevant conclusions.

II. Blass matrix

The Blass matrix is a simple multiplex transmission line network, firstly introduced in [27] as a new approach to the radiation of stacked beams by multidirectional antennas. Basically, the Blass matrix is a series feeding technique, to excite the radiating elements of a linear array, which are connected to the feedline by directional couplers. Fig. 1 shows a scheme representing the principle of operation of a Blass matrix designed to radiate M beams (corresponding to the M imput terminals on the rows) with a linear array consisting of N antennas (corresponding to the N output terminals on the columns). The remaining terminals of each row and of each column are connected to adapted loads, as it is depicted in Fig. 1. So, the Blass matrix consists of $M \times N$ phase shifters and of $M \times N$ directional couplers. The directional coupler is a four-port component, as it is depicted in Fig. 2. Each port has a coupled port, with coupling value C_{mn}, a direct port, with coupling value $\sqrt{1-C_{mn}^2}$, and an isolated port [36]. Referring to Fig. 2 and assuming port 1 as the input port, port 2 is the coupled port, port 3 is the direct port and port 4 is the isolated port. In the same way, if port 4 is assumed as the input port, port 3 is the coupled port, port 2 is the direct port and port 1 is the isolated port.

Now, given M desired beams, the Blass matrix design consists in determining the $M \times N$ coupling values C_{mn} and the $M \times N$ phase shifter values φ_{mn}, in such a way that the n–th array element is excited with a proper excitation a_{mn} to radiate the m–th desired beam.

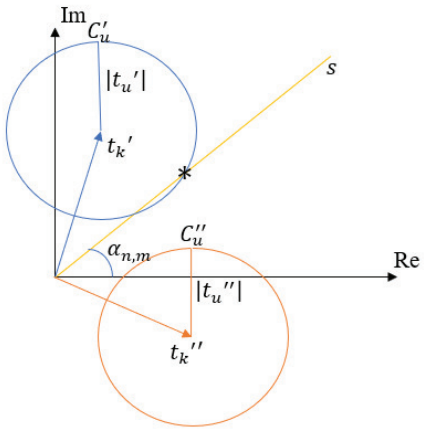

Fig. 3. Graphical representation of the two possible cases for the summation in (7) on the Gauss plane, when condition (3) is imposed. Blue circumference corresponds to a feasible problem, red circumference corresponds to unfeasible problem.

In this work, the problem of beam steering is addressed, thus only the direction of the main beam is considered. Moreover, in order to have a very simple and versatile structure, which is a mandatory issue in 5G systems, the branch line is used as directional coupler. Thus, $C_{mn} = C = 1/\sqrt{2}$, for $m = 1, \ldots, M, n = 1, \ldots, N$. So, here, the design objective is to determine all the $M \times N$ phase shifter values φ_{mn}, which allow the array to point the beam toward the desired direction θ_m, for $m = 1, \ldots, M$.

III. Design Procedure

The first step of the design procedure consists in evaluating all the transmission coefficients T_{mn}, from the generic input port m to the generic output port n. Now, it is worth spending some more words on the principle of operation of the Blass matrix. In fact, it is evident that the wave traveling from an input port $m > 1$ is affected by the presence of the feedline(s) placed above it, and may reach the n–th radiating element through different paths. The design procedure proposed in this paper rigorously takes into account all the secondary paths from input m to output n to correctly evaluate the transmission coefficient T_{mn}, which is used to derive the final values of the phase shifters, as it is described in details below.

Consider a uniform linear antenna array (ULA) consisting of N isotropic elements placed on the z axis at the positions $z_n = nd, n = 1, \ldots, N$, being d the inter-element distance. The radiation pattern of the ULA can be expressed as [37]:

$$F_m(\theta) = \sum_{n=1}^{N} a_{mn} \exp(jnkd\cos\theta), \tag{1}$$

where $k = 2\pi/\lambda$ is the wave number and λ is the wavelength, θ is the angle from the array axis and $\mathbf{a}_m = [a_{m1}, a_{m2}, \ldots, a_{mN}]$ is the excitation vector. Now, it is well known that in order to point the beam toward a desired

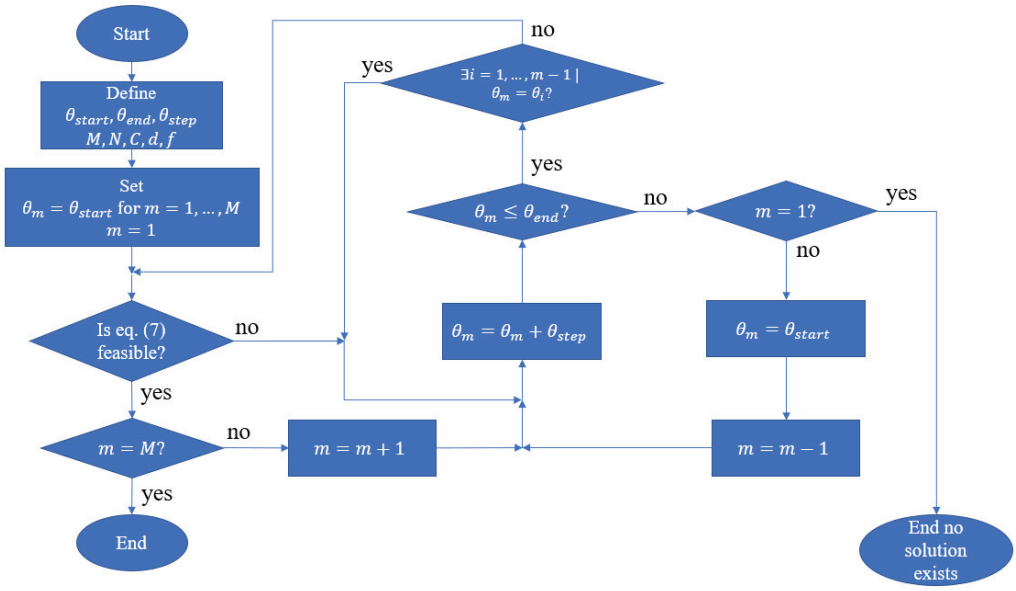

Fig. 4. Flowchart of the proposed design procedure.

direction θ_m, the excitation phases $\alpha_{mn} = \angle a_{mn}$ may be selected for $m = 1, \dots, M,\ n = 1, \dots, N$ as [37]:

$$\alpha_{mn} = -(n-1)kd\cos\theta_m. \tag{2}$$

Imposing that the values given by (2) be the phases of the Blass matrix transmission coefficients according to equation:

$$\angle T_{mn} = \alpha_{mn} \tag{3}$$

allows one to derive the phase shifter values φ_{mn} as follows.

In fact, let start with the first row, corresponding to the input $m = 1$. The wave travelling from the first input port to the nth output port passes through exactly n directional couplers, with direct paths through $n-1$ directional couplers and a coupled path through the last coupler. Thus, the generic transmission coefficient T_{1n}, is derived as:

$$T_{1n} = C\left(\sqrt{1-C^2}\right)^{n-1}\exp(-j\varphi_{1n}),\ n = 1, \dots, N. \tag{4}$$

Imposing condition (3) in (4), gives the first-row phase values:

$$\varphi_{1n} = -\alpha_{1n}, \quad n = 1, \dots, N. \tag{5}$$

Then, consider the transmission coefficient with m=2, n=1:

$$T_{21} = C\sqrt{1-C^2}\ \exp[-j(\varphi_{21} + \varphi_{11})]. \tag{6}$$

Imposing condition (3) to T_{21} in (6), allows one to easily derive the unknown value φ_{21}.

Now, as stated above, the complexity increases when $m, n > 1$, due to the presence of secondary paths from input m to output n. So, considering for example $m = n = 2$, there are two different paths that connect these two ports. The first path passes through the phase shifters φ_{21} and φ_{12}, with transmission coefficient $t_k = C^3\exp[-j(\varphi_{21} + \varphi_{12})]$, which has already been evaluated (the subscript k stands for known). The second path passes through the phase shifters φ_{22} and φ_{12}, with transmission coefficient $t_u = \left(\sqrt{1-C^2}\right)^2 C\exp[-j(\varphi_{22} + \varphi_{12})]$, containing the unknown phase φ_{22} (the subscript u stands for unknown). Analogously, proceeding row by row, the generic transmission coefficient T_{mn} can always be expressed as the following summation:

$$T_{mn} = t_k + t_u, \tag{7}$$

where t_k is the transmission coefficient of all the paths passing through phase shifters which have already been evaluated, whereas t_u is the transmission coefficient of the only path passing through the unknown phase shifter φ_{mn}, which can be identified by imposing condition (3) to (7).

However, it is here demonstrated that condition (3) is sometimes not realizable, when the coupling value C is fixed in advance. In fact, consider Fig. 3, where two possible situations are depicted on the complex plane for the transmission coefficient T_{mn} in (7). The vectors t'_k and t''_k represent two possible values of the known component of the summation in (7), whose unknown component has an amplitude ($|t'_u|$ and $|t''_u|$, respectively) which is determined by the coupling value C. Thus, the circumferences C'_u and C''_u represent all the possible values for the transmission coefficient T_{mn} in the two considered cases. The straight line s contains all the points that satisfy condition (3). So, it is evident that in the blue case a solution for φ_{mn} can be chosen, which is given by the intersection point between s and C'_u, which maximizes the transmission coefficient (represented by an asterisk in Fig. 3). On the contrary, in the red case, $C''_u \cap s = \emptyset$. This means that equation (7) has no solution when condition (3) is imposed. This implies that the pointing angle θ_m can not be realized. Of course, as it is evident from Fig. 3, this non-feasibility

also depends on the known component of the transmission coefficient, thus on the previous rows of the Blass matrix. This observation suggests that a proper design procedure might exist to find a set of M feasible pointing directions, eventually by simply changing the order of the matrix rows.

Now, suppose that an ULA consisting of N elements with assigned inter-element distance d and working frequency f is required to point the beam toward M directions belonging to the sector $[\theta_{\text{start}}, \theta_{\text{end}}]$. In order to find a set of M feasible pointing directions θ_m when the coupling value C is fixed in advance, the following design procedure is proposed, which is graphically depicted in Fig. 4 and validated in the next section.

Step 1 Set $\theta_m = \theta_{\text{start}}$ for $m = 1, \ldots, M$, $m = 1$.

Step 2 For $n = 1, \ldots, N$ evaluate T_{mn} and solve (7) imposing (3). If a solution exists, go to Step 3, else go to Step 4.

Step 3 If $m = M$ all the phase values have been successfully evaluated and the Blass matrix design has been completed. Stop. Else set $m = m + 1$ and go to Step 4.

Step 4 Set $\theta_m = \theta_m + \theta_{\text{step}}$. If $\theta_m \leq \theta_{\text{end}}$ go to Step 5, else go to Step 6.

Step 5 If there is $i = 1, \ldots, m-1$ such that $\theta_m = \theta_i$, go to Step 4. Else go to Step 2.

Step 6 If $m = 1$ the problem is unfeasible. Stop. Else, set $\theta_m = \theta_{\text{start}}$, $m = m - 1$, go to Step 4.

In words, the proposed procedure is developed to find a predefined number M of feasible pointing angles, which belong to the desired angular sector. With the developed algorithm, the angular sector $[\theta_{\text{start}}, \theta_{\text{end}}]$ is discretized with the user-defined step θ_{step}. In comparison with the algorithm in [29], the proposed procedure is less flexible, as here the pointing directions can not be arbitrarily chosen, and they finally belong to a discrete set of directions. As explained above, this limitation is due to the choice of adopting the same directional coupler in the entire feeding network. On the other hand, the algorithm proposed in [29] optimizes not only the phases, but also all the coupling values of the Blass matrix. Of course, this choice offers more degrees of freedom and thus improves the results, but at the expenses of a more complex structure. To conclude, in the authors' opinion, both the algorithm and the resulting Blass matrix structure proposed in this paper are simpler and cheaper than those in [29]. Next section shows an example of application.

IV. Results

In order to prove the effectiveness of the proposed synthesis method, a Blass matrix with $M = N = 4$ is here considered. More precisely, the ULA is composed by $N = 4$ isotropic radiators having $d = 0.6\lambda$, which corresponds to $d = 30$ mm at the carrier frequency $f = 6$ GHz. The branch line is assumed as directional coupler, having $C = 1/\sqrt{2}$. Finally, $M = 4$ pointing directions are calculated using the algorithm presented in Fig. 4 with $\theta_{\text{start}} = 50°$, $\theta_{\text{step}} = 5°$ and $\theta_{\text{end}} = 180°$.

The obtained pointing angles are listed in the second column of Table I, along with the element phases α_{mn}, which allow to realize the beam pointing and are evaluated by (2). It is

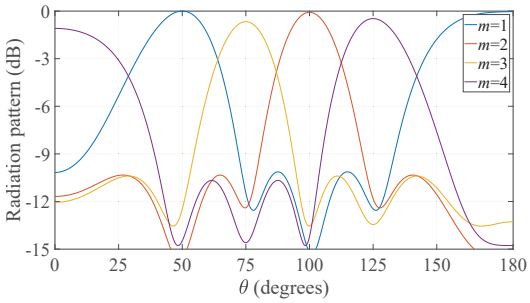

Fig. 5. Radiation patterns of the multidirectional antenna with the designed feeding network.

TABLE I
POINTING ANGLES θ_m EVALUATED BY THE DESIGN PROCEDURE PROPOSED IN FIG. 4 AND ELEMENT PHASES α_{mn} EVALUATED BY (2).

m	θ_m	$n=1$	$n=2$	$n=3$	$n=4$
1	50°	0°	221°	82°	303°
2	100°	0°	37°	75°	112°
3	125°	0°	123°	247°	11°
4	75°	0°	304°	248°	192°

to be noted that if the same pointing angles are sequentially considered (i.e., if $\theta_m < \theta_{m+1}, m = 1, 2, 3$), the procedure to evaluate the Blass matrix phase shifters fails to find a solution for φ_{43} and φ_{44} (which corresponds to the red case of Fig. 4). But, when the algorithm described in the previous section is applied, the problem can be solved for all the phase shifters of the Blass matrix, which are here reported in Table II.

Finally, Table III lists the amplitudes of the $M \times N$ transmission coefficients T_{mn} obtained for the designed Blass matrix, and Fig. 5 shows the normalized patterns obtained by setting $a_{mn} = |T_{mn}| \exp(j\alpha_{mn})$ in (1). As it can be seen from Fig. 5, the desired pointing angles are properly realized, so proving the effectiveness of the proposed design procedure. The high sidelobes arising at the array axis for the pointing angles which are furthest from broadside are due to the high element spacing ($d > \lambda/2$), which has been chosen to simulate a real situation, where patch antennas must be physically located on the PCB substrate, for example. However, when real radiators are used instead of ideal isotropic antennas, these high pattern sidelobes are lowered thanks to the element patterns.

V. Conclusion

Passive multibeam antennas are one of the key technological aspects to enable the capabilities required to 5G systems. The algorithm proposed in this paper has the aim of designing a Blass matrix, which can be fully integrated with the elements

TABLE II
BLASS MATRIX: DESIGNED PHASE SHIFTER VALUES φ_{mn}.

m	$n=1$	$n=2$	$n=3$	$n=4$
1	0°	221°	82°	303°
2	0°	90°	233°	148°
3	0°	263°	220°	190°
4	0°	180°	217°	0°

TABLE III
BLASS MATRIX: AMPLITUDES OF THE TRANSMISSION COEFFICIENT T_{mn}.

m	$n=1$	$n=2$	$n=3$	$n=4$
1	0.7071	0.5000	0.3536	0.2500
2	0.5000	0.7058	0.2500	0.3394
3	0.3536	0.2193	0.6773	0.4267
4	0.2500	0.3752	0.4386	0.6506

of an ULA into a single substrate of a common PCB. The Blass matrix phase shifters are simply implemented as delay microstrip transmission lines having suitable lengths. Identical branch lines are used as directional couplers, which are extremely simple microstrip four-port components.

Then, it is shown that, fixing the coupling values in advance, may fail to realize some specific beams, thus reducing the versatility of this feeding technique. So, an original algorithm has been developed to evaluate a prescribed number of feasible pointing directions belonging to an angular sector of interest. The effectiveness of the overall design procedure is proved by a numerical example, involving an ULA consisting of four radiating elements and realizing four different beams.

REFERENCES

[1] A. Gupta and R. K. Jha, "A Survey of 5G Network: Architecture and Emerging Technologies." *IEEE Access*, vol. 3, pp. 1206–1232, 2015.

[2] A. I. Sulyman et al., "Radio Propagation Path Loss Models for 5G Cellular Networks in the 28 GHz and 38 GHz Millimeter-Wave Bands." *IEEE Commun. Mag.*, vol. 52, no. 9, pp. 78-86, Sep. 2014.

[3] M. R. Akdeniz et al., "Millimeter Wave Channel Modeling and Cellular Capacity Evaluation." *IEEE J. Sel. Areas Commun.*, vol. 32, no. 6, pp. 1164-1179, Jun. 2014.

[4] J. Lota, S. Sun, T. S. Rappaport, and A. Demosthenous, "5G Uniform Linear Arrays With Beamforming and Spatial Multiplexing at 28, 37, 64, and 71 GHz for Outdoor Urban Communication: A Two-Level Approach." *IEEE Trans. Veh. Technol.*, vol. 66, no. 11, pp. 9972-9985, Nov. 2017.

[5] S. Chen and J. Zhao, "The Requirements, Challenges, and Technologies for 5G of Terrestrial Mobile Telecommunication." *IEEE Communun. Mag.*, vol. 52, no. 5, pp. 36–43, May 2014.

[6] A.A. Althuwayb, "Low-Interacted Multiple Antenna Systems Based on Metasurface-Inspired Isolation Approach for MIMO Applications." *Arab. J. Sci. Eng.*, pp. 1-10,May 2021.

[7] M. Alibakhshikenari et al., "A Comprehensive Survey on "Various Decoupling Mechanisms With Focus on Metamaterial and Metasurface Principles Applicable to SAR and MIMO Antenna Systems"." *IEEE Access*, vol. 8, pp. 192965-193004, 2020.

[8] M. Alibakhshikenari et al., "A Comprehensive Survey of "Metamaterial Transmission-Line Based Antennas: Design, Challenges, and Applications"." *IEEE Access*, vol. 8, pp. 144778-144808, Aug. 2020.

[9] M. Mohammadi Shirkolaei, "Wideband linear microstrip array antenna with high efficiency and low side lobe level". *Int. J. RF Microw. Comp.-Aided Eng.*, pp. 1-7, Aug. 2020.

[10] M. Alibakhshikenari, B. S. Virdee, A. A. Althuwayb, F. Falcone and E. Limiti, "Interaction Suppression Technique for High-Density Antenna Arrays for mm-Wave 5G MIMO Systems." In *15th EuCAP*, pp. 1-5, Mar. 2021.

[11] M. Mohammadi Shirkolaei and J. Ghalibafan, "Scannable Leaky-Wave Antenna Based on Ferrite-Blade Waveguide Operated Below the Cutoff Frequency." *IEEE Trans. Magn.*, vol. 57, no. 4, pp. 1-10, Apr. 2021.

[12] M. Alibakhshikenari, B.S. Virdee and E. Limiti, "Study on Isolation and Radiation Behaviours of a 34×34 Array-Antennas Based on SIW and Metasurface Properties for Applications in Terahertz Band Over 125–300 GHz." *Optik*, vol. 206, pp. 1-10, Mar. 2020.

[13] M. Mohammadi Shirkolaei, "High Efficiency X-Band Series-Fed Microstrip Array Antenna." *Progr. Electromagn. Res. C*, vol. 105, pp. 35-45, Aug. 2020.

[14] M. Alibakhshikenari et al., "Isolation Enhancement of Densely Packed Array Antennas with Periodic MTM-Photonic Bandgap for SAR and MIMO Systems." *IET Microw. Ant. Propag.*, Mar. 2019.

[15] M. Alibakhshikenari, B.S. Virdee, C.H. See, R.A. Abd-Alhameed, F. Falcone and E. Limiti, "Surface Wave Reduction in Antenna Arrays Using Metasurface Inclusion for MIMO and SAR Systems." *Radio Sci.*, vol. 54, pp. 1067-1075, Oct. 2019.

[16] M. Alibakhshikenari et al., "Mutual-Coupling Isolation Using Embedded Metamaterial EM Bandgap Decoupling Slab for Densely Packed Array Antennas." *IEEE Access*, vol. 7, pp. 51827-51840, Apr. 2019.

[17] M. Alibakhshikenari et al., "Mutual Coupling Suppression Between Two Closely Placed Microstrip Patches Using EM-Bandgap Metamaterial Fractal Loading." *IEEE Access*, vol. 7, pp. 23606-23614, Feb. 2019.

[18] M. Alibakhshikenari et al., "Interaction Between Closely Packed Array Antenna Elements Using Meta-Surface for Applications Such as MIMO Systems and Synthetic Aperture Radars." *Radio Sci.*, vol. 53, no. 11, pp. 1368-1381, Nov. 2018.

[19] M. Alibakhshikenari et al., "Antenna Mutual Coupling Suppression Over Wideband Using Embedded Periphery Slot for Antenna Arrays." *Electronics*, vol. 7, no. 9, pp. 1-11, Sept. 2018.

[20] M. Alibakhshikenari et al., "Study on Isolation Improvement Between Closely-Packed Patch Antenna Arrays Based on Fractal Metamaterial Electromagnetic Bandgap Structures." *IET Microw. Ant. Propag.*, vol. 12, no. 14, pp. 2241-2247, Nov. 2018.

[21] M.M. Kamal MM et al., "A Novel Hook-Shaped Antenna Operating at 28 GHz for Future 5G mmwave Applications." *Electronics*, vol 10, no. 6, Mar. 2021.

[22] M. Mohammadi, F.H. Kashani, J. Ghalibafan, "A Partially Ferrite-Filled Rectangular Waveguide With CRLH Response and its Application to a Magnetically Scannable Antenna." *J. Magn. and Magn. Mater.*, vol. 491, pp. 1-9, Dec. 2019.

[23] A. Ghaffar et al., "Design and Realization of a Frequency Reconfigurable Multimode Antenna for ISM, 5G-Sub-6-GHz, and S-Band Applications. 2021, 11." *Appl. Sci.*, vol. 11, no. 4, pp. 1-14, Feb. 2021.

[24] F. Babich, M. Comisso, and R. Corrado, "On the Impact of the Video Quality Assessment in 802.11e Ad-Hoc Networks Using Adaptive Retransmissions", in *IEEE Med-Hoc-Net*, pp. 1 - 8, Jun. 2014.

[25] J. Butler and R. Lowe, "Beamforming Matrix Simplifies Design of Electronically Scanned Antennas." *Electron. Des.*, vol. 9, pp. 170–173, Apr. 1961.

[26] A. Tajik, A. Shafiei Alavijeh and M. Fakharzadeh, "Asymmetrical 4×4 Butler Matrix and its Application for Single Layer 8×8 Butler Matrix." *IEEE Trans. Antennas Propag.*, vol. 67, no. 8, pp. 5372-5379, Aug. 2019.

[27] J. Blass. "Multidirectional Antenna a New Approach to Stacked Beam." *IRE Int. Con. Rec.*, vol. 1, pp. 48–50, Mar. 1960.

[28] F. Casini, R. Vincenti Gatti, L. Marcaccioli, R. Sorrentino "A Novel Design Method for Blass Matrix Beam-Forming Networks." In *37th EuMC*, Oct. 2007.

[29] S. Mosca, F. Bilotti, A. Toscano, and L. Vegni, "A Novel Design Method for Blass Matrix Beam-Forming Networks." *IEEE Trans. Antennas Propag.*, vol. 50, no. 2, pp. 225–232, Feb. 2002.

[30] T. Djerafi, N. J. G. Fonseca, and K. Wu, "Planar Ku-band 4×4 Nolen Matrix in SIW Technology." *IEEE Trans. Microw. Theory Techn.*, vol. 58, no. 2, pp. 259–266, Feb. 2010.

[31] N. J. G. Fonseca, "Printed S-band 4×4 Nolen Matrix for Multiple Beam Antenna Applications," *IEEE Trans. Antennas Propag.*, vol. 57, no. 6, pp. 1673–1678, Jun. 2009.

[32] W. Rotman and F. Turner "Wide-Angle Microwave Lens for Line Source Applications." *IEEE Trans. Antennas Propag.*, vol. 11, no. 6, pp. 623–632, Nov. 1963.

[33] K. K. Chan and S. K. Rao, "Design of a Rotman Lens Feed Network to Generate a Hexagonal Lattice of Multiple Beams," *IEEE Trans. Antennas Propag.*, vol. 50, no. 8, pp. 1099–1108, Aug. 2002.

[34] W. Hong et al., "Multibeam Antenna Technologies for 5G Wireless Communications." *IEEE Trans. Antennas Propag.*, vol. 65, no. 12, pp. 6231-6249, Dec. 2017.

[35] D.I. Lialios et al., "Design of True Time Delay Millimeter Wave Beamformers for 5G Multibeam Phased Arrays." *Electronics*, Aug. 2020.

[36] D.M. Pozar, *Microwave Engineering.* 3rd ed. Hoboken, NJ, USA: Wiley, 2005.

[37] C.A. Balanis. *Antenna Theory.* 3rd ed. Hoboken, NJ, USA: Wiley, 2005.